

## Low energy lepton scattering: recent results for electron and positron interactions

**Stephen J Buckman<sup>1</sup>, Todd Maddern<sup>2</sup>, Jessica Francis-Staite<sup>2</sup>, Leigh Hargreaves<sup>2</sup>, Michael J Brunger<sup>2</sup>, Gustavo Garcia<sup>3</sup>, Julian C. Lower<sup>1</sup>, Subhendu Mondal<sup>1</sup>, James P Sullivan<sup>1</sup>, Adric Jones<sup>1</sup>, Peter Caradonna<sup>1</sup>, Daniel Slaughter<sup>1</sup>, Casten Mackochekanwa<sup>1</sup>, Robert P McEachran<sup>1</sup>**

<sup>1</sup>ARC Centre for Antimatter-Matter Studies, Research School of Physical Sciences and Engineering, College of Science, Australian National University, Canberra, ACT, Australia

<sup>2</sup>ARC Centre for Antimatter-Matter Studies SOCPES, Flinders University, GPO Box 2100, Adelaide, SA, Australia

<sup>3</sup>Instituto de Física Fundamental, CSIC, Serrano 113-bis, 28006, Madrid, Spain

Stephen.buckman@anu.edu.au

**Abstract.** This report will review several new experimental developments for low energy (1-50 eV) scattering of both electrons and positrons from atoms and molecules. Experiments include an apparatus for studies of scattering from unstable molecular radicals, a position- and time-sensitive time-of-flight spectrometer for studies of near threshold electronic excitation of atoms and molecules and a trap-based positron scattering experiment for measurements of low energy positron scattering from rare gas atoms. Where possible, comparisons are also made with other experimental determinations and with contemporary scattering theory.

### 1. Introduction

Electron and positron interactions with atoms, molecules and materials can provide important insights into reaction dynamics, atomic and molecular structure and a wealth of both realized and potential applications in technology, biomedical science and the environment. At low energies, electron interactions are characterized by, amongst other things, strong scattering resonances involving the temporary trapping of the projectile in the field of the atom or molecule. These resonances often lead to profound effects on the scattering cross sections and, in some cases, can enhance scattering rates for vibrational excitation, for example, by orders of magnitude. For molecular systems they also lead to a very important process known as dissociative attachment whereby the negative ion complex decays via dissociation, resulting in many cases in the production of reactive neutral and negative ion species. This process is known to be important in areas as diverse as radiation damage of DNA and its constituent molecules [1] and the production of reactive etch products in fluorocarbon feedstock gases used in plasma processing [2].

Measurements of positron interactions, on the other hand, are not so extensive, or advanced, as those for their matter counterpart. Positron scattering experiments have until recently lacked the specificity and accuracy of electron scattering measurements, mainly as a consequence of low beam intensities and/or relatively poor energy resolution. A significant advance in recent years has been the

advent of trap-based positron beams which, when combined with new techniques developed for charged particle scattering in large magnetic fields, have enabled many new measurements. For example, the improved energy resolution and sensitivity offered by these techniques have enabled the first absolute scattering measurements for excitation processes in atoms and molecules, including the direct measurement of positronium formation (see [3] for a recent review of positron interactions). These techniques promise much new fundamental information on positron interactions with atoms and molecules, including measurements on biologically important molecules which may have relevance for a deeper understanding of the interactions that underpin diagnostic techniques such as Positron Emission Tomography (PET).

For both electron and positron scattering, another important rationale for the measurements lies in the comparison with state of the art quantum scattering theory. In order for theory to develop, particularly in the case of complex molecular targets, it is imperative that accurate ‘benchmark’ experimental measurements are available for comparison.

In the following sections we discuss several new experimental initiatives in electron and positron physics. First we describe a new apparatus and initial results for electron interactions with molecular radical species. We then describe a technique which, in principle, can provide benchmark measurements for near-threshold electron impact electronic excitation of atoms and molecules. Finally we consider the development of a new positron trap and scattering experiment and results that have been obtained with it for positron scattering from the rare gases.

## 2. Scattering of electrons by molecular radicals

There is an increasing realization that molecular radicals play an important role in a range of electron-induced processes, from radiation damage in tissue, to plasma processing and deposition technologies. In the latter case, fluorocarbon feedstock gases are commonly used as the etching gas but in the discharge environment, electron-induced dissociation readily results in the production of  $CF_x$  radicals which in turn undergo a range of collision processes with other discharge constituents, including the electrons. In the present study we have used a pyrolytic source in combination with a pulsed supersonic nozzle to create a beam of  $CF_2$  molecular radicals, from which we have studied elastic electron scattering. Some of these results have been reported previously [4].

The apparatus used to perform the  $CF_2$  cross section measurements has been described in a recent publication [5] and we will not repeat that detail here. Briefly, the experiment is a crossed-beam electron scattering experiment comprising four differentially pumped chambers. The first chamber contains the solenoid valve, the pyrolytic nozzle, and the skimmer, and is pumped by a 10 in. diffusion pump. The second chamber, separated from the first by the skimmer, houses 9 fixed-angle electron detectors, spanning an angular range of 20–135 deg., and is pumped by a 156 l/s turbomolecular pump. The third chamber contains the electron monochromator, and is differentially pumped by a 50 l/s turbomolecular pump. The fourth chamber, separated from the second by a 30-mm aperture, houses a time-of-flight mass spectrometer (TOFMS) and is evacuated by a 6 inch diffusion pump.

Following pyrolysis, the heated products in the beam undergo cooling through supersonic expansion. A skimmer, placed downstream from the pyrolytic nozzle, serves to collimate the beam for passage through the scattering chamber. The electron monochromator produces a monoenergetic electron beam which is scattered from the molecular beam, and an array of 9 fixed-angle detectors is used to determine the scattering intensities for those angles. The composition of the beam is monitored by the TOFMS with 118-nm radiation used to ionize species through single-photon ionization. The temperature of the pyrolysis nozzle is measured with an optical pyrometer. Differential cross section (DCS) data were placed on an absolute scale by using a modified form of the skimmed supersonic relative density method (SSRDM) [6]. A schematic of the experimental layout is shown in Figure 1.

Examples of the first such results for low energy electron scattering from  $CF_2$  are given in Figure 2. Here we compare the present absolute differential cross sections with several theoretical predictions at

incident electron energies of 30 and 40 eV. The level of agreement is remarkably good, given the difficulty of both the experimental measurements and the theoretical calculations.

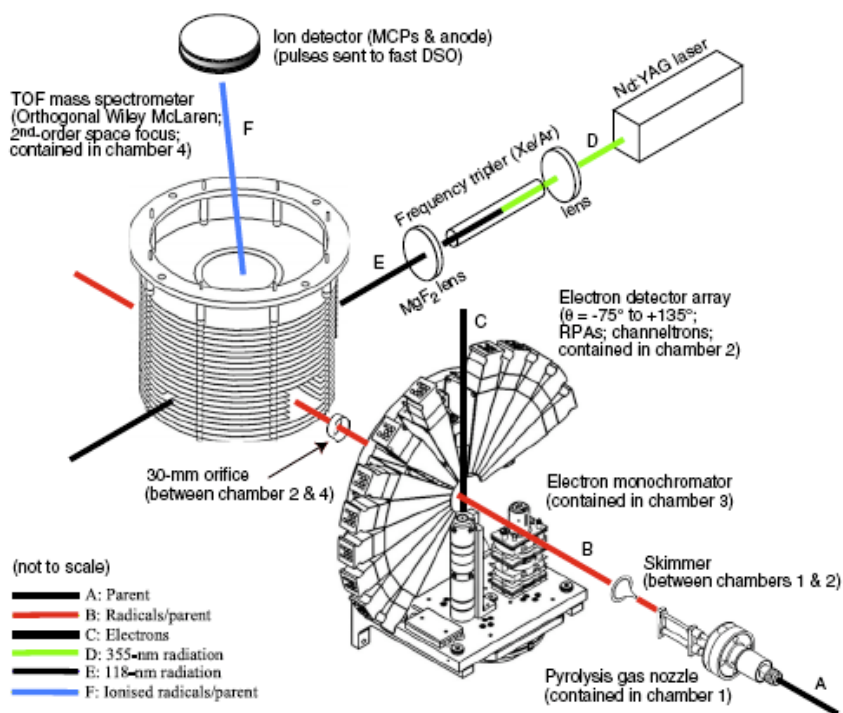


**Figure 1:** Schematic layout of the molecular radicals scattering experiment.

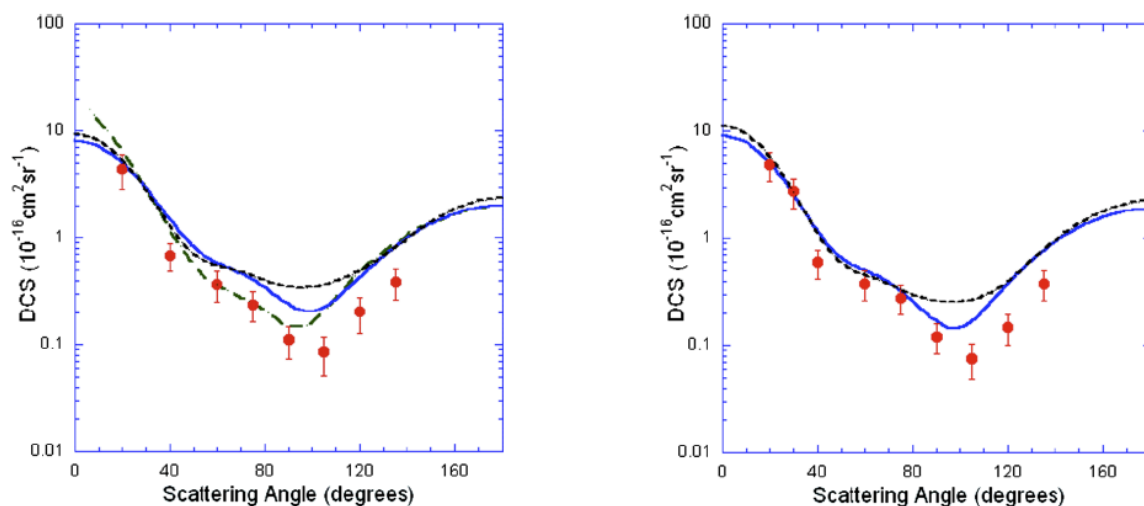


**Figure 2:** Absolute differential cross sections for elastic scattering from the  $\text{CF}_2$  radical at energies of 30 eV (left) and 40 eV (right). The solid line is a Schwinger variational calculation at the static exchange level, the short dashed line the same calculation with polarization included [4] and the long dashed line the ISM-DWA calculation of [7].

### 3. Near-threshold electronic excitation of atoms and molecules

Electronic excitation can lead to the production of photons, metastable species or dissociative products, including free radicals, and as such it is an important process which is widely exploited in a range of technological devices. At near-threshold energies the cross sections for these processes are often enhanced by the presence of resonances. Somewhat paradoxically perhaps, the accuracy of much of the experimental data available in the literature for such processes is, at times, rather poor, if one takes the level of agreement between various experiments as a gauge. In large part this is due to experimental and/or analysis difficulties.

This energy region within a few electron volts of threshold represents a challenge experimentally as measurements typically require high-resolution electron monochromators and analysers and some means for establishing the absolute magnitude of the scattering cross sections. The most commonly used approach has been to measure the flux of inelastically scattered electrons, for a particular scattering channel and scattering angle, relative to that for the elastic scattering intensity at the same incident energy and scattering angle. If the transmission of the energy analysing device is known, the inelastic scattering cross section can be readily determined from the ratio of scattered electron intensities, providing the elastic cross section is well known. The main experimental issue that has to be resolved is usually the determination of the transmission of the energy analysing device (e.g., a hemispherical analyser) as a function of the scattered electron energy. In the present work we have employed a time-of-flight technique to ensure uniform transmission of the scattered electrons.

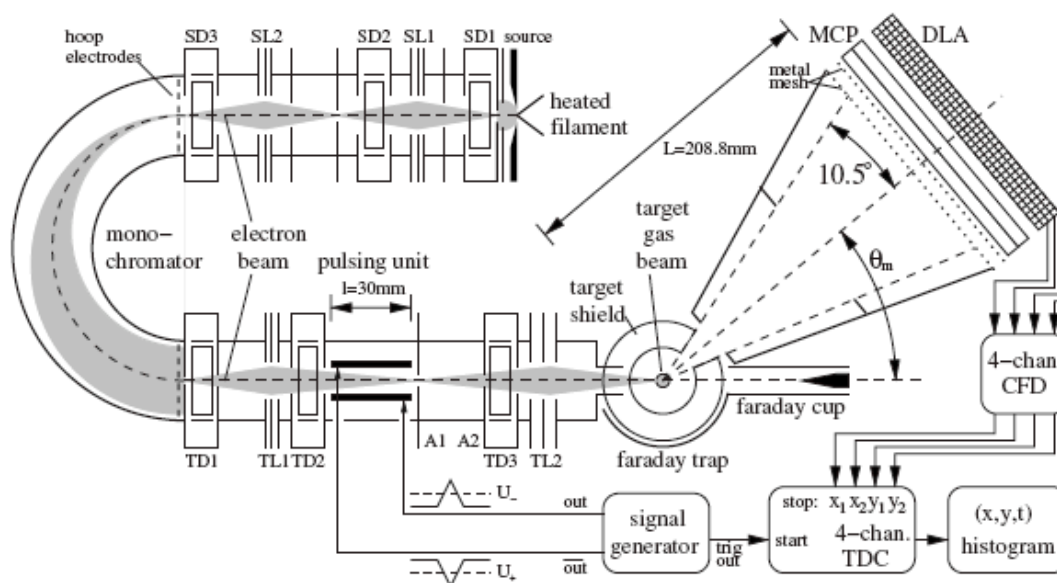


**Figure 3:** Schematic diagram of ToF apparatus.

The experimental arrangement consists of a crossed electron-molecular beam configuration, with the incident electron beam produced from an electrostatic monochromator. The target beam is formed by effusive flow of helium or  $N_2$  through a single capillary tube. The energy of the incident beam is readily tuneable and calibrated, in the present case, by measuring well-known resonance features in metastable atom/molecule excitation functions. These measurements also indicate that the energy resolution of the incident beam is typically around 100 meV, with a CW beam current of several nA. We use a time-of-flight (ToF) energy analyser as the dispersive element for the scattered electron analysis. Scattered electrons are allowed to drift for 20 cm in a field free environment before being accelerated and striking a large area position sensitive detector comprising an 80 mm diameter channel plate and delay-line anode (Röntdek DLD-80). Scattered electrons can be simultaneously detected

over a range of scattering angles of about  $22^\circ$  and, by measuring their time-of-flight, their energy can also be determined. The mean scattering angle is varied by changing the position of the electron monochromator, which is mounted on a rotating turntable. As the experiment involves the measurement of electron flight times, a pulsed beam of several ns duration (FWHM) is formed by sweeping the beam, in a controlled fashion, across a small defining aperture. Space does not permit a full description of the apparatus here but further details can be found elsewhere [8,9]. A schematic layout of the experiment is given in Figure 3.

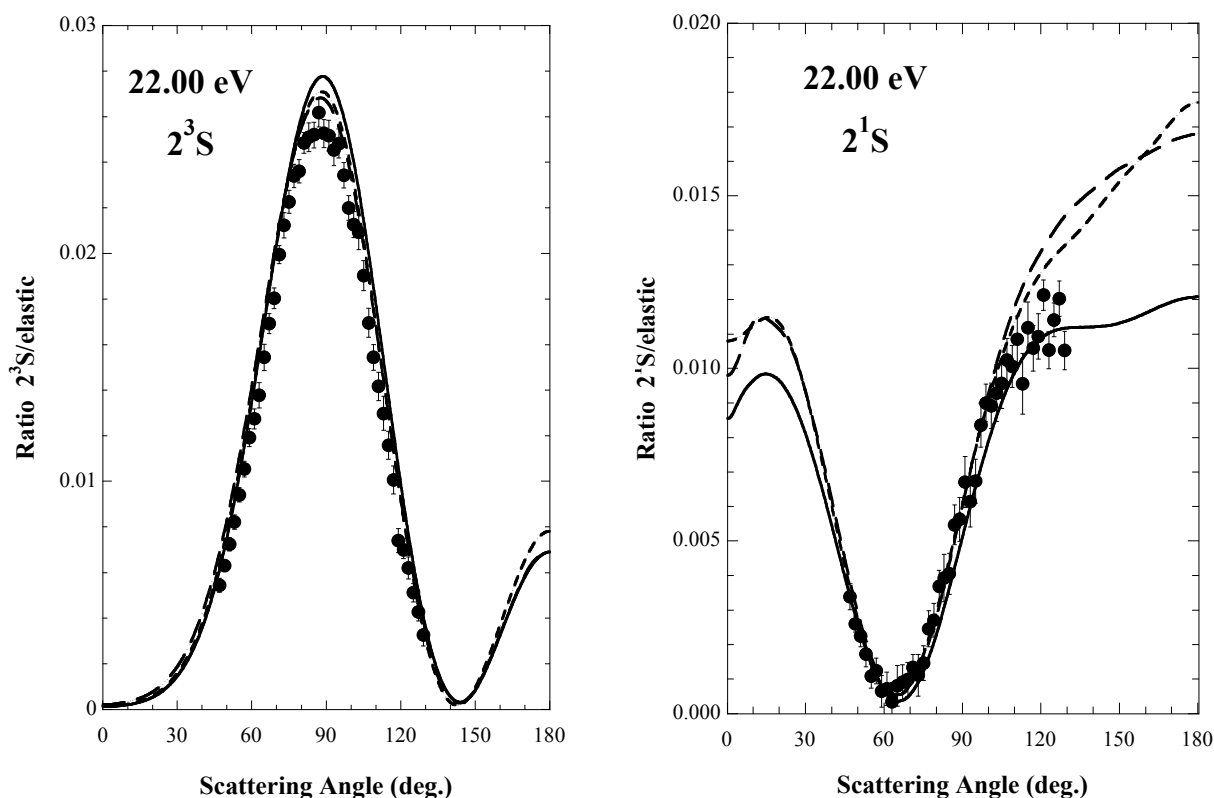


**Figure 4:** Near threshold excitation of Helium  $n=2$  levels by 22 eV electrons. The solid line is the convergent close coupling calculation [13], the short dashed line the RMPS calculation [14], and the long dashed line the B-spline R-Matrix theory [15]

We have measured differential scattering cross sections for near-threshold energies for several excited states in He and  $N_2$ , using this new apparatus. Examples of these measurements are provided in Figures 4-6. The measurements for helium provide a good test of the bona fides of the apparatus and technique as helium is one system where contemporary scattering theory has achieved an extremely high level of accuracy for a range of elastic, inelastic and ionizing events following electron impact. This is demonstrated in Figure 4 where for the first two  $n=2$  states of helium we see excellent agreement between the present measurements for the ratio of the elastic to inelastic scattering probabilities, and the results from three theoretical calculations.

In the case of  $N_2$  (Figures 5 and 6) there are serious discrepancies in the literature for the values of the near-threshold cross sections for a number of low-lying excited levels and for incident electron energies within about 10 eV of threshold (see [10] for the most recent discussion of these issues). Our preliminary results indicate some differences in the experimental cross sections with those of [10] at 10 eV incident energy, but significantly better agreement is found at 15 eV. For example, at 10 eV the

total inelastic scattering intensity measured in the present experiment (Figure 5) is somewhat higher than that of [10], although many of the individual excited state cross sections which are unfolded from this data show good agreement (see for example Figure 6, left panel). At 15 eV the agreement in both the total inelastic scattering intensity, and the individual excited state components of this, is considerably better. In general the present results at 15 eV are in better agreement with the recent experiment of [10] than with older determinations of the individual excited state cross sections [eg. 11,12].

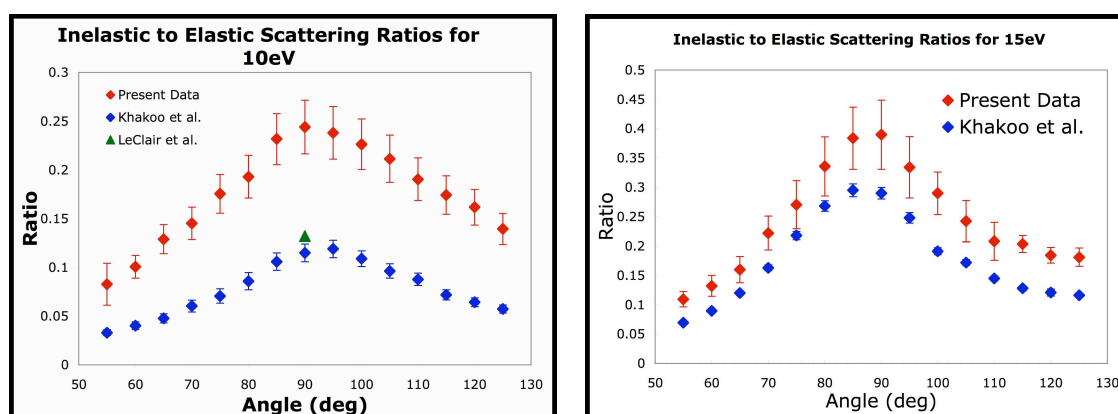


**Figure 5:** Ratio of total inelastic to elastic scattering intensity for  $N_2$  at incident energies of 10 and 15 eV. The present data are compared with the measurements of [10].

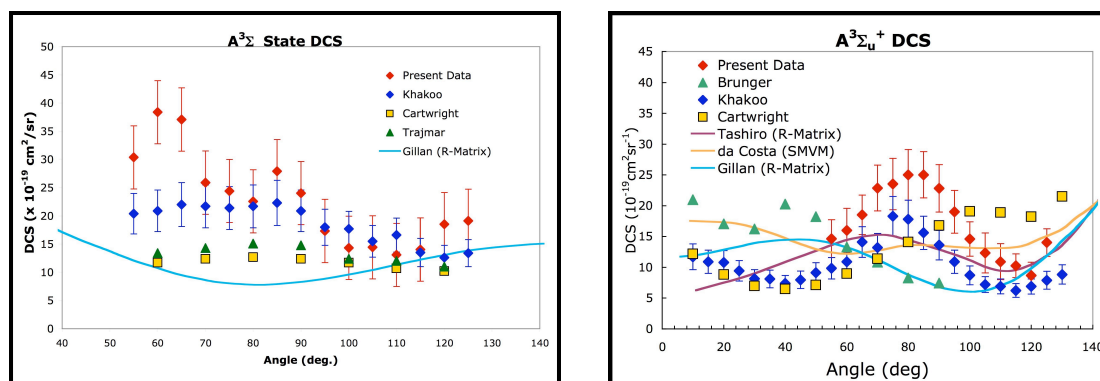


**Figure 6:** Differential cross sections for the excitation of the  $A^3\Sigma_u^+$  state of  $N_2$  at incident energies of 10 and 15 eV.

#### 4. Low energy positron scattering

The advent of high-resolution, trapped-based beams of positrons [16] has revealed many new opportunities for fundamental studies of positron interactions with atoms and molecules. Now it is possible to produce relatively intense, pulsed, variable energy beams of positrons with energy widths considerably less than 100 meV. Such positron sources have enabled energy resolved measurements of elastic and inelastic scattering cross sections, including processes such as vibrational and electronic excitation [17].

We have developed a new, trap-based beam of positrons based on the approach pioneered by Surko and collaborators at the University of California, San Diego. This beam uses positrons from a  $\sim 25$  mCi  $^{22}\text{Na}$  source, which are magnetically guided, trapped and collisionally cooled in a Surko trap and then released in a pulsed beam with an energy width of  $\sim 60$  meV and with a controlled, but readily varied, energy. The pulsed beam is incident on a gas cell containing the target of interest and the energy of the positrons after the scattering cell is analysed with a simple, but highly effective, retarding potential analyzer, before they are detected by a channel plate detector. This technique of scattering in a high magnetic field has been described in considerable detail elsewhere [17], and we do not repeat that detail here. It offers some significant advantages in sensitivity over conventional techniques and enables direct measurements of important quantities such as total, total elastic, total inelastic and total positronium formation cross sections.

An example of preliminary data from this apparatus is shown in Figure 7, where we illustrate measurements of the total positron scattering cross section for neon and compare it with one previous experimental determination and a recent theoretical calculation. The calculation [18] uses the polarized orbital technique. The agreement in the region of the Ramsauer-Townsend minimum is very good between all three cross sections, while at higher energies, discrepancies of the order of 20% exist between all three, up to the positronium formation threshold at 14.76 eV, where the cross section shows a marked increase due to the opening of this important inelastic channel.

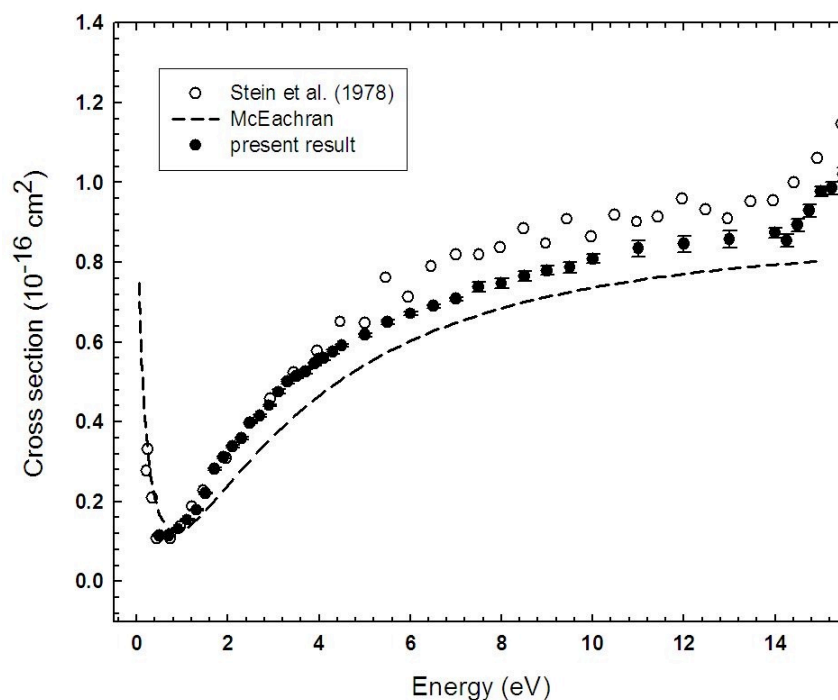


**Figure 7:** Total scattering cross section for positrons interacting with neon atoms.

## 5. Conclusions and future directions

This review of recent cross section measurements for low energy lepton scattering has attempted to highlight a number of significant and recent experimental advances in the field. These have led to new, exciting results that have the potential to establish a series of ‘benchmarks’ for electron collisions with targets which could not be studied previously, such as molecular radicals, and processes for which there exist substantial discrepancies in the literature, such as near-threshold electronic excitation. In addition, new techniques developed for low energy positron scattering are

providing similar opportunities to benchmark these collision processes. Future work in these areas will involve an extension of studies to other molecular radicals, potentially  $\text{CF}_3$  and  $\text{CH}_2$ , the extension of the ToF technique to more complex polyatomic molecules such as  $\text{H}_2\text{O}$  and  $\text{CO}_2$ , and the application of the new positron facilities to a broad range of collision measurements on atoms and molecules.

### Acknowledgements

It is a pleasure to acknowledge the support of the Australian Government through the Australian Research Council's Centre of Excellence program and the Department of Innovation, Industry, Science and Research's International Science Linkages Program.

### References

- [1] Boudaiffa B, Cloutier P, Hunting D, Huels M A and Sanche L 2000 *Science* **287** 1658
- [2] National Research Council I 1996 *Database Needs for Modelling and Simulation of Plasma Processing* (New York: National Academy Press)
- [3] Surko C M, Gribakin G F and Buckman S J 2005 *J. Phys. B: At. Mol. Opt. Phys.* **38** R57
- [4] Maddern T M, Hargreaves L R, Francis-Staite J R, Brunger M J, Buckman S J, Winstead C and McKoy V 2008 *Phys. Rev. Lett.* **100** 063202
- [5] Maddern T M, Hargreaves L R, Bolarizadeh M, Brunger M J and Buckman S J 2008 *Meas. Sci. Technol.* **19** 085801
- [6] Hargreaves L R, Francis-Staite J R, Maddern T M, Brunger M J and Buckman S J 2007 *Meas. Sci. Technol.* **18** 2783
- [7] Lee M-T, Machado L E, Brescansin L M, Castro E A and de Souza G L 2006 *Phys. Rev. A* **74** 052716
- [8] Lange M, Matsumoto J, Lower J, Buckman S, Zatsarinny O, Bartschat K, Bray I and Fursa D 2006 *J. Phys. B: At. Mol. Opt. Phys.* **39** 4179
- [9] Lange M, Matsumoto J, Setiawan A, Panajotovic R, Harrison J, Lower J C, Newman D S, Mondal S and Buckman S J 2008 *Rev. Sci. Instrum.* **79** 043105
- [10] Khakoo M A, Johnson P V, Ozkay I, Yan P, Trajmar S and Kanik I 2005 *Phys. Rev. A* **71** 062703
- [11] Cartwright D C, Chutjian A, Trajmar S, and Williams W 1977 *Phys. Rev. A* **16**, 1013
- [12] Brunger M J and Teubner P J O 1990 *Phys. Rev. A* **41** 1413
- [13] Fursa D and Bray I 1995 *Phys. Rev. A* **52** 1279 and see reference [8]
- [14] Bartschat K, Hudson E T, Scott M P, Burke P G and Burke M V 1996 *Phys. Rev. A* **54** R998 and see reference [8]
- [15] Zatsarinny O and Bartschat K 2004 *J. Phys. B: At. Mol. Opt. Phys.* **37** 2173 and see reference [8]
- [16] Gilbert S J, Kurz C, Greaves R G and Surko C M 1997 *Appl. Phys. Lett.* **70** 1944
- [17] Sullivan J P, Gilbert S J, Marler J P, Greaves R G, Buckman S J and Surko C M 2002 *Phys. Rev. A* **66** 042708
- [18] McEachran R P and Stauffer A D 2008 Private Communication